

Morphology-dependent resonances of spherical droplets with numerous microscopic inclusions

Michael I. Mishchenko,^{1,*} Li Liu,^{1,2} and Daniel W. Mackowski³

¹NASA Goddard Institute for Space Studies, 2880 Broadway, New York, New York 10025, USA

²Department of Applied Physics and Applied Mathematics, Columbia University, 2880 Broadway, New York, New York 10025, USA

³Department of Mechanical Engineering, Auburn University, Alabama 36849, USA

*Corresponding author: michael.i.mishchenko@nasa.gov

Received February 4, 2014; accepted February 12, 2014;
posted February 13, 2014 (Doc. ID 205997); published March 14, 2014

We use the recently extended superposition T -matrix method to study the behavior of a sharp Lorenz–Mie resonance upon filling a spherical micrometer-sized droplet with tens and hundreds of randomly positioned microscopic inclusions. We show that as the number of inclusions increases, the extinction cross-section peak and the sharp asymmetry-parameter minimum become suppressed, widen, and move toward smaller droplet size parameters, while ratios of diagonal elements of the scattering matrix exhibit sharp angular features indicative of a distinctly nonspherical particle. Our results highlight the limitedness of the concept of an effective refractive index of an inhomogeneous spherical particle. © 2014 Optical Society of America

OCIS codes: (290.0290) Scattering; (260.5740) Resonance; (290.4020) Mie theory; (290.4210) Multiple scattering; (290.5850) Scattering, particles.

<http://dx.doi.org/10.1364/OL.39.001701>

Micrometer-sized droplets with numerous microscopic inclusions represent an important morphological type of scattering objects [1–9] as well as a great modeling challenge. Until a few months ago, computations of electromagnetic scattering by such particles had to rely on the simplest model of a droplet with only one inclusion [2,5,7,8,10] or on approximate approaches such as various effective-medium theories (EMTs) [11], the Monte Carlo ray-tracing technique [12,13], and the degenerate perturbation method [9]. The recent extension of the superposition T -matrix method (STMM) to arbitrarily clustered and nested spherical domains [14] is a major breakthrough that makes possible numerically exact computations of electromagnetic scattering for realistically large droplets with hundreds of inclusions. Hence, the primary objectives of this Letter are to report representative STMM results and analyze the effects of multiple randomly positioned inclusions on the scattering properties of a micrometer-sized spherical droplet. As a secondary objective, we use our numerical data to discuss and illustrate the inherent limitedness of the concept of an effective refractive index.

The STMM has three key qualities that make it ideal for this study. First, it is a direct computer solver of the frequency-domain macroscopic Maxwell equations and as such involves no approximations. Second, it is highly accurate and thus can be used to study the finest details of electromagnetic scattering patterns unattainable with other techniques [15,16]. Third, the analytical orientation averaging procedure serves as an extremely efficient and accurate means of modeling the statistically uniform distribution of inclusions inside the spherical host. Indeed, the brute-force way to suppress modeling “noise” requires averaging over tens or hundreds of thousands of discrete realizations of the droplet interior. With the STMM, one can use just one quasi-random configuration of the inclusions because subsequent analytical averaging over all orientations of this configuration captures,

in essence, an infinite continuous set of realizations and yields noise-free curves unambiguously revealing the actual effects of random internal inhomogeneity (cf. [17]). We will demonstrate later that the results thus obtained are virtually independent of the initial set of positions of the inclusions provided that they are chosen using a “sufficiently random” coordinate-generation procedure.

Perhaps the most striking trait of electromagnetic scattering by a homogeneous, perfectly spherical droplet is the existence of morphology-dependent resonances (MDRs) [18–20]. The black solid curves in Figs. 1(a) and 1(b) show the extinction cross section and asymmetry parameter, respectively, as functions of the droplet size parameter $X = 2\pi R/\lambda$ computed at a wavelength of $\lambda = 0.55 \mu\text{m}$ for a homogeneous spherical droplet with a varying radius R and a fixed refractive index of $m_d = 1.31$. Both curves reveal a narrow Lorenz–Mie MDR centered at the size parameter $X_{\text{res}} \approx 32.5832$ ($R_{\text{res}} \approx 2.85218 \mu\text{m}$). It is well known that such sharp resonances are very fragile and are easily destroyed by minute deviations of the droplet shape from that of a perfect sphere [21,22]. It is, therefore, quite interesting to examine the behavior of this MDR upon filling the drop with an increasing number N of randomly positioned spherical inclusions.

The color solid curves in Figs. 1(a) and 1(b) show the orientation-averaged STMM results for $N = 10, 30, \dots, 300$ randomly positioned inclusions having a fixed size parameter $x = 1$ (corresponding to a radius of $r \approx 0.08754 \mu\text{m}$) and a fixed refractive index $m_i = 1.55$. The initial quasi-random configuration of N nonoverlapping inclusions was created using a simple random-number coordinate generator. It is quite obvious that there are three major effects of increasing N : the Lorenz–Mie MDR becomes increasingly suppressed, widens, and moves toward smaller values of the droplet size parameter. For comparison, the dotted curves depict the results of computations based on the Maxwell–Garnett

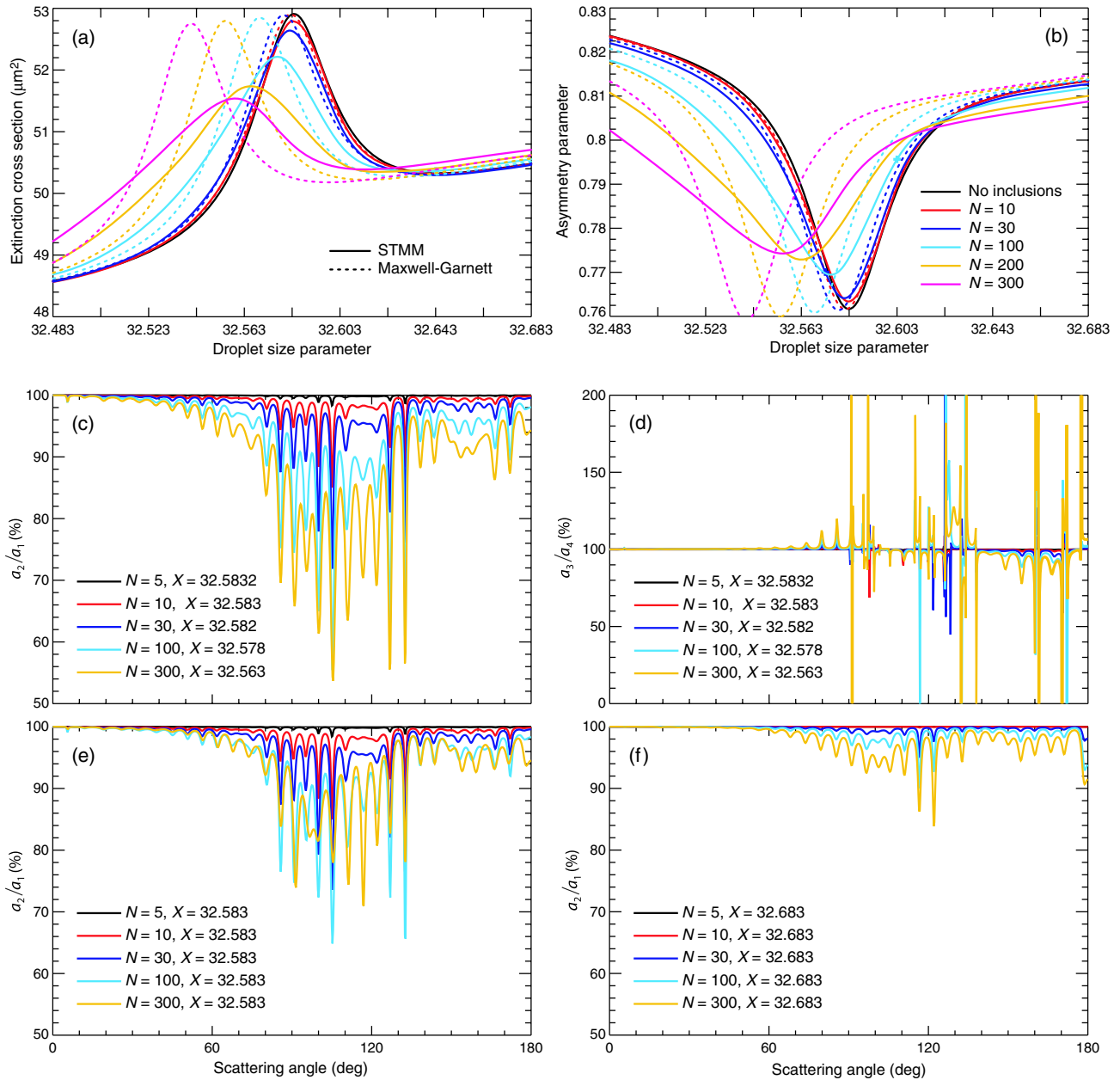


Fig. 1. (a), (b) Extinction cross section and asymmetry parameter for a spherical droplet with N randomly positioned inclusions. (c)–(f) As in (a), (b) but for ratios of the elements of the Stokes scattering matrix.

effective-medium approximation (MGA) [11]. Since the size parameter of the inclusions is kept constant, the MGA refractive index varies as the droplet size parameter increases from 32.483 to 32.683. To plot the dotted curves in Figs. 1(a) and 1(b), we computed the MGA refractive index for droplet size parameters $X \in [32.483, 32.683]$ in steps of 0.001. The Bruggeman-approximation (BA) results are virtually identical to the MGA ones and thus are not shown.

The first effect of increasing N in Figs. 1(a) and 1(b) is consistent with the results of laboratory measurements reported in [4]. It is in fact remarkable that as small a volume fraction of the inclusions as 0.87% (for $N = 300$) serves to reduce the height of the extinction peak (relative to its right-hand wing) by a factor exceeding two. The third effect is qualitatively consistent with the MGA trend. However, the MGA obviously overstates the rate

of the effective refractive index change with increasing N and, more importantly, does not predict the very suppression of the MDR by the inclusions.

To illustrate the invariance of the STMM results with respect to the choice of the initial configuration of the inclusions, we plot in Fig. 2 the asymmetry parameter computed by averaging over orientations of two different initial configurations shown in Fig. 3 and obtained by running the random-number coordinate generator twice. It is seen indeed that the resulting curves are hardly distinguishable even for the relatively small number of inclusions $N = 30$ and can be expected to be even closer for larger values of N (see, e.g., the bottom panels in Fig. 12 of [23]).

The angular distribution and the polarization state of the scattered light are typically described in terms of the normalized Stokes scattering matrix

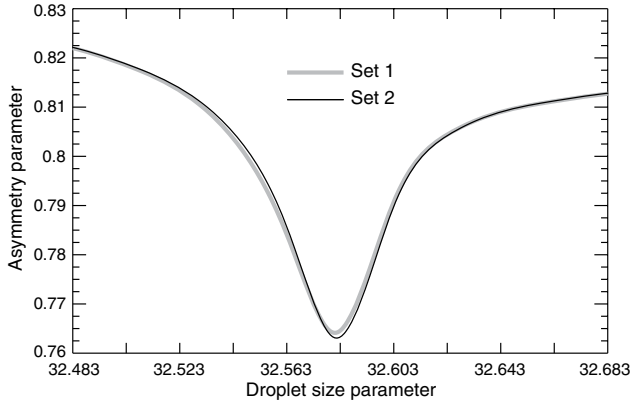


Fig. 2. Asymmetry parameter computed for two different realizations of the initial configuration of 30 inclusions.

$$\tilde{\mathbf{F}}(\Theta) = \begin{bmatrix} a_1(\Theta) & b_1(\Theta) & 0 & 0 \\ b_1(\Theta) & a_2(\Theta) & 0 & 0 \\ 0 & 0 & a_3(\Theta) & b_2(\Theta) \\ 0 & 0 & -b_2(\Theta) & a_4(\Theta) \end{bmatrix}, \quad (1)$$

where $\Theta \in [0^\circ, 180^\circ]$ is the angle between the incidence and scattering directions [20]. The (1,1) element of $\tilde{\mathbf{F}}(\Theta)$ is the conventional phase function satisfying the normalization condition

$$\frac{1}{2} \int_0^\pi d\Theta \sin \Theta a_1(\Theta) = 1. \quad (2)$$

Two unique properties of a homogeneous, perfectly spherical particle are the identities

$$a_2(\Theta)/a_1(\Theta) \equiv 1 \quad \text{and} \quad a_3(\Theta)/a_4(\Theta) \equiv 1. \quad (3)$$

It is obvious that any EMT always reproduces these identities provided that the surface of the host is perfectly spherical.

Figures 1(c) and 1(d) show the results of STMM computations of the ratios $a_2(\Theta)/a_1(\Theta)$ and $a_3(\Theta)/a_4(\Theta)$ for a spherical droplet with different numbers of inclusions. The specific size parameters of the host droplet correspond to the maxima in the respective extinction curves in Fig. 1(a). First and foremost, the data in Figs. 1(c) and 1(d) reveal fundamental violations of the identities (3), thereby further illustrating the limitedness of the concept of effective refractive index. Second, increasing N serves to strengthen the sharp extrema in the $a_2(\Theta)/a_1(\Theta)$ and $a_3(\Theta)/a_4(\Theta)$ curves, whereas its effect in Figs. 1(a) and 1(b) was just the opposite. The origin of the remarkable

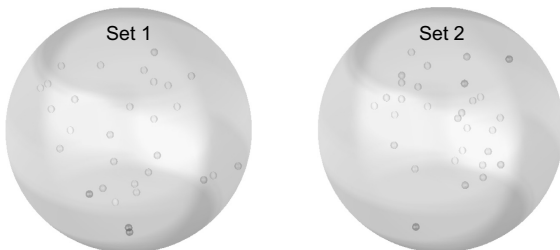


Fig. 3. Two different realizations of the initial configuration of 30 inclusions used in Fig. 2.

stability of the locations of the numerous sharp extrema in Figs. 1(c) and 1(d) with increasing N is not immediately obvious to us. All in all, our results imply that measurements of the ratios $a_2(\Theta)/a_1(\Theta)$ and $a_3(\Theta)/a_4(\Theta)$ can be extremely sensitive indicators of the presence of inclusions in otherwise spherical droplets.

In Fig. 1(e), the ratio $a_2(\Theta)/a_1(\Theta)$ is plotted for $X = 32.583$ corresponding to the location of the Lorenz–Mie MDR for a homogeneous droplet. Comparison with Fig. 1(c) shows an obvious reduction in the depths of the sharp minima. Furthermore, the deepest minima are no longer caused by the droplet with $N = 300$ inclusions. This behavior of the ratio $a_2(\Theta)/a_1(\Theta)$ is quite intriguing and may not have a straightforward qualitative explanation. It does appear to imply, however, that the sharp angular features in Figs. 1(c) and 1(d) are caused by strong interactions of the individual inclusions with a quasi-homogeneous spherical host droplet characterized by a “resonance effective refractive index” that is somewhat greater than 1.31 but smaller than that predicted by the MGA. This conjecture may be corroborated by Fig. 1(f) which seems to imply that the alleged interactions become even weaker for the droplet size parameter $X = 32.683$ corresponding to the right-hand wing of the Lorenz–Mie resonance.

In summary, our numerically exact STMM results reveal several profound effects of microscopic inclusions on a narrow Lorenz–Mie MDR of a micrometer-sized spherical droplet. The suppression of the extinction cross section and asymmetry-parameter resonances with increasing N and their shift toward smaller droplet size parameters can be understood, at least qualitatively. The deviations of the ratios $a_2(\Theta)/a_1(\Theta)$ and $a_3(\Theta)/a_4(\Theta)$ from unity are also consistent with the droplet inhomogeneity lacking spherically symmetric structure. However, the cause of the specific traits of the sharp angular extrema revealed by these ratios and their dependence on the droplet size parameter may not necessarily be obvious.

Chýlek *et al.* [11] state explicitly that EMTs are *ad hoc* approximations based on heuristic shortcuts and are not derived explicitly from the macroscopic Maxwell equations. As a consequence, the accuracy of such derived effective refractive indices and the precise conditions for their permissible use are often difficult to assess. Our STMM results represent the first morphologically relevant test of EMTs based on a direct numerically exact solution of the Maxwell equations. It is evident that the MGA and BA have largely failed this particular test. However, this does not necessarily mean that EMTs cannot perform better in situations less demanding than computations for perfectly spherical host droplets in the vicinity of a sharp Lorenz–Mie resonance.

We thank Steven Hill for providing his computer program for the calculation of Lorenz–Mie MDR locations and widths [24]. This material is based upon work supported by the NASA Remote Sensing Theory Program managed by Lucia Tsaoussi and the NASA Radiation Sciences Program managed by Hal Maring. The majority of numerical results were obtained with the “Discover” supercomputer at the NASA Center for Climate Simulation.

References

1. P. Chýlek, D. Ngo, and R. G. Pinnick, *J. Opt. Soc. Am. A* **9**, 775 (1992).
2. M. Mazumder, S. C. Hill, and P. W. Barber, *J. Opt. Soc. Am. A* **9**, 1844 (1992).
3. B. V. Bronk, M. J. Smith, and S. Arnold, *Opt. Lett.* **18**, 93 (1993).
4. D. Ngo and R. G. Pinnick, *J. Opt. Soc. Am. A* **11**, 1352 (1994).
5. P. Chýlek, G. B. Lesins, G. Videen, J. G. D. Wong, R. G. Pinnick, D. Ngo, and J. D. Klett, *J. Geophys. Res.* **101**, 23365 (1996).
6. G. Videen, P. Pellegrino, D. Ngo, J. S. Videen, and R. G. Pinnick, *Appl. Opt.* **36**, 6115 (1997).
7. G. Videen, W. Sun, Q. Fu, D. R. Secker, R. S. Greenaway, P. H. Kaye, E. Hirst, and D. Bartley, *Appl. Opt.* **39**, 5031 (2000).
8. D. R. Prabhu, M. Davies, and G. Videen, *Opt. Express* **8**, 308 (2001).
9. P.-T. Leung, S.-W. Ng, K.-M. Pang, and K.-M. Lee, *Opt. Lett.* **27**, 1749 (2002).
10. K. A. Fuller, *Opt. Lett.* **19**, 1272 (1994).
11. P. Chýlek, G. Videen, D. J. W. Geldart, J. S. Dobbie, and H. C. W. Tso, in *Light Scattering by Nonspherical Particles: Theory, Measurements, and Applications*, M. I. Mishchenko, J. W. Hovenier, and L. D. Travis, eds. (Academic, 2000), p. 273.
12. M. I. Mishchenko and A. Macke, *J. Quant. Spectrosc. Radiat. Transfer* **57**, 767 (1997).
13. L. Liu, M. I. Mishchenko, S. Menon, A. Macke, and A. A. Lacis, *J. Quant. Spectrosc. Radiat. Transfer* **74**, 195 (2002).
14. D. W. Mackowski, *J. Quant. Spectrosc. Radiat. Transfer* **133**, 264 (2014).
15. M. I. Mishchenko, J. W. Hovenier, W. J. Wiscombe, and L. D. Travis, in *Light Scattering by Nonspherical Particles: Theory, Measurements, and Applications*, M. I. Mishchenko, J. W. Hovenier, and L. D. Travis, eds. (Academic, 2000), p. 29.
16. F. M. Kahnert, *J. Quant. Spectrosc. Radiat. Transfer* **79–80**, 775 (2003).
17. M. I. Mishchenko, L. Liu, D. W. Mackowski, B. Cairns, and G. Videen, *Opt. Express* **15**, 2822 (2007).
18. P. Chýlek, *J. Opt. Soc. Am.* **66**, 285 (1976).
19. S. C. Hill and R. E. Benner, in *Optical Effects Associated with Small Particles*, P. W. Barber and R. K. Chang, eds. (World Scientific, 1988), p. 3.
20. M. I. Mishchenko, L. D. Travis, and A. A. Lacis, *Scattering, Absorption, and Emission of Light by Small Particles* (Cambridge University, 2002).
21. M. I. Mishchenko and A. A. Lacis, *Appl. Opt.* **42**, 5551 (2003).
22. J. M. Dlugach and M. I. Mishchenko, "Effects of nonsphericity on the behavior of Lorenz–Mie resonances in scattering characteristics of liquid-cloud droplets," *J. Quant. Spectrosc. Radiat. Transf.* (to be published).
23. M. I. Mishchenko, *Rev. Geophys.* **46**, RG2003 (2008).
24. S. C. Hill, C. K. Rushforth, R. E. Benner, and P. R. Conwell, *Appl. Opt.* **24**, 2380 (1985).